*Far East J. Appl. Math.* **21**(1) (2005), 31-41

# LINEAR STABILITY OF PULSATILE SLIP FLOWS IN MICROCHANNELS

**FRANCESCO FEDELE and DARREN L. HITT**

GEST & GMAO, Code 610.5
NASA Goddard Space Flight Center
Greenbelt, MD 20771, U. S. A.

Department of Mechanical Engineering
University of Vermont
Burlington, VT 05405 U. S. A.

## Abstract

We examine the linear stability to axisymmetric disturbances in weakly rarefied flows ('slip regime') in microchannels. A semi-analytical solution of the Orr-Sommerfeld equation shows that pulsatile flow is linearly stable in the slip regime although a sudden change in the stability properties of the flow occurs at a critical value of the Knudsen number $\mathrm{Kn}_{cr} = (2-\sigma)/8\sigma$, where $\sigma$ is the accommodation coefficient. Flow structures corresponding to the largest energy growth are toroidal vortex tubes that are transported diffusively and convectively by the mean flow. Transient energy growth is found to decrease for Knudsen numbers $\mathrm{Kn} < \mathrm{Kn}_{cr}$ due to the diminished wall vorticity induced by the slip conditions. Thus the Orr-Sommerfeld operator for slip flow is less non-normal compared to continuum-based no-slip flows.



## 1. Introduction

The study of pulsatile tube flow, first considered in the context of arterial hemodynamics in the mid-1950s [5], has found renewed

2000 Mathematics Subject Classification: Primary 76E05.

Key words and phrases: slip flow, stability, pulsatile pipe flow, Orr-Sommerfeld operator, Galerkin projection, non-normality, vortex tubes, energy growth.

Received April 21, 2005

significance in its application to MEMS microfluidic engineering applications. A feature common to many of the devices described in the microfluidics literature that incorporate 'chip-level' pumping is that the flow is pulsatile in nature [4], [10]. On the micro- and nano-scale the surface roughness of the channel walls can have greater impact on the flow behavior in contrast to their macro-scale counterparts; this is especially true for the case of rarefied (or 'slip') flows [7]. In addition to the potential generation of flow disturbances, the surface roughness also influences the velocity boundary condition for rarefied flows through tangential momentum accommodation coefficient $\sigma$ [1].

Linear stability analyses of continuum-regime steady [2] and pulsatile flows [3], [11] show that all of the eigenmodes are damped, although an initial energy growth of the flow perturbation can occur due to the non-normality of the Orr-Sommerfeld operator [8], [9]. Transient growth is important if transition to turbulence is thought as emanating from 'by-pass transition' mechanisms [9]. In the following we extend the previous studies on pulsatile flow stability to the case of weakly rarefied flows ('slip regime') defined by Knudsen numbers $\leq 0.3$.

## 2. Orr-Sommerfeld Equation for a Weakly Rarefied Pulsatile Flow

We consider as an undisturbed state the fully-developed, pulsatile flow in a pipe of circular cross section of radius $R$ driven by an imposed periodic pressure gradient $\partial P/\partial z$. The fully-developed streamwise velocity $W(r, t)$ satisfies the following initial boundary value problem

$$\rho \frac{\partial W}{\partial t} - \mu \frac{1}{r} \frac{\partial}{\partial r}\left( r \frac{\partial W}{\partial r} \right) = -\frac{\partial P}{\partial z}, \quad \frac{\partial P}{\partial z} = -[K_0 + K_\omega \exp(i\omega t)], \tag{1}$$

where $\mu$ is the dynamic viscosity, $\rho$ is the density and $\omega$ is the frequency of the oscillating pressure gradient. For a weakly rarefied flow (or 'slip regime'), the velocity boundary condition is modeled as a first-order slip condition [6]

$$W|_{r=R} = \frac{2-\sigma}{\sigma} \lambda \frac{\partial W}{\partial r}\bigg|_{r=R}, \tag{2}$$

where $\lambda$ is the gas mean free path and $\sigma$ is the tangential momentum

coefficient (TMAC). The first-order slip condition (2) is valid provided the Knudsen number of the flow $\mathrm{Kn} \equiv \lambda/2R \leq 0.3$ [6]. The value of $\sigma$ is restricted to the range of $[0, 1]$ whose lower and upper limits correspond to 'pure-slip' and 'no-slip,' respectively. The precise value of $\sigma$ depends upon the fluid and the surface properties of the channel walls. Recent experiments by Arkilic et al. [1] using nitrogen, argon and carbon-dioxide and polished, single-crystal silicon walls have suggested a range of $\sigma = 0.75 - 0.85$.

The analytical solution of (1) subject to the boundary condition (2), when properly non-dimensionalized, is found as

$$W(r, t) = W_0 + W_1 \exp(it\ \mathrm{St}), \tag{3}$$

$$W_0(r) = 1 - r^2 + 4\left(\frac{2-\sigma}{\sigma}\right)\mathrm{Kn}, \tag{4}$$

$$W_1(r, t) = \frac{4K_\omega}{i\,\mathrm{St}\,\mathrm{Re}\,K_0}\left[1 - \frac{1}{1 - \left(2\frac{2-\sigma}{\sigma}\mathrm{Kn}\right)i^{3/2}\mathrm{Wo}\dfrac{J_1(i^{3/2}\mathrm{Wo})}{J_0(i^{3/2}\mathrm{Wo})}}\frac{J_0(i^{3/2}\mathrm{Wo}\,r)}{J_0(i^{3/2}\mathrm{Wo})}\right], \tag{5}$$

where the velocity scale is based on the steady Poiseuille flow component $(= K_0R^2/4\mu)$, the length scale is the tube diameter, and the time scale is the oscillation period. The quantities Re and St are the Reynolds number and Strouhal numbers, respectively,

$$\mathrm{Re} = \frac{\rho U R}{\mu} \qquad \mathrm{St} = \frac{2R\omega}{U} \tag{6}$$

and are related to the Womersley number, $\mathrm{Wo} = \sqrt{\mathrm{ReSt}}$. The latter is generally interpreted as the ratio of oscillatory inertia to viscous forces.

We define a cylindrical coordinate system with $z$-axis along the streamwise direction and impose an axisymmetric velocity perturbation to the basic flow. Introducing a Stokes stream function of the form $\Psi(r, z, t) = \psi(r, t)e^{i\alpha z}$, with $\alpha$ the streamwise wavenumber, radial and

streamwise velocity components of the perturbation are given by

$$u = -\frac{1}{r}\frac{\partial \Psi}{\partial z} = -\frac{\psi(r, t)}{r} i\alpha e^{i\alpha z}, \quad w = \frac{1}{r}\frac{\partial \Psi}{\partial r} = \frac{1}{r}\frac{\partial \psi}{\partial r} e^{i\alpha z} \tag{7}$$

and the condition of incompressibility is automatically satisfied. Substitution of the basic flow (3)-(5) and the perturbation velocity (7) into the general Navier-Stokes equations yields, after neglecting nonlinear terms, the following Orr-Sommerfeld equation for the stream function $\psi$ in dimensionless form [3]

$$\mathcal{L}\psi_t - Wi\alpha^3\psi + i\alpha(-\psi\mathcal{L}W + W\mathcal{L}\psi) = \mathrm{Re}^{-1}\mathcal{L}^2\psi, \tag{8}$$

where $\mathcal{L}$ is defined by $\mathcal{L} = \partial^2/\partial r^2 - r^{-1}\partial/\partial r - \alpha^2$. The boundedness of the flow at the centerline and the slip condition at the wall of the pipe provide the boundary conditions:

$$\frac{1}{r}\psi, \quad \frac{1}{r}\frac{\partial \psi}{\partial r} < \infty, \quad r \to 0^+, \tag{9}$$

$$\psi = 0, \quad \frac{1}{r}\frac{d\psi}{dr} = 2\left(\frac{2-\sigma}{\sigma}\right)\mathrm{Kn}\frac{d}{dr}\left(\frac{1}{r}\frac{d\psi}{dr}\right), \quad r = 1. \tag{10}$$

## 3. Galerkin Projection Method

We solve the Orr-Sommerfeld equation (8) by seeking an approximation stream function $\hat{\psi}(r, t)$ as

$$\hat{\psi}(r, t) = \sum_{k=1}^{N} a_k(t)\phi_k(r), \tag{11}$$

where $\{a_k(t)\}_{n=1}^{N}$ are time-dependent coefficients to be determined and the basis $\{\phi_n(r)\}_{n=1}^{\infty}$ is the set of eigenfunctions of the long-wave limit $(\alpha \to 0)$ of the Orr-Sommerfeld equation (8). These basis functions satisfy the eigenvalue problem [3]

$$\widetilde{\mathcal{L}}^2\phi_n = -\mathrm{Re}\lambda_n\widetilde{\mathcal{L}}\phi_n \tag{12}$$

subject to the boundary conditions (9)-(10). Here, $\widetilde{\mathcal{L}} = r\partial/\partial r\,(r^{-1}\partial/\partial r)$ is a reduced operator and the eigenvalues are given by $\lambda_n = \chi_n^2/\mathrm{Re}$, where

$\chi_n$ are the roots of the eigenvalue relation

$$J_2(\chi) - 2s\mathrm{Kn}\chi J_1(\chi) = 0, \quad s = \frac{2-\sigma}{\sigma}, \tag{13}$$

and where $J_1(r)$ and $J_2(r)$ are the Bessel functions of first kind of order 1 and 2, respectively. One readily finds the solution for $\phi_n$ as

$$\phi_n(r) = \frac{\sqrt{2}r\left(r - \dfrac{J_1(\chi_n r)}{J_1(\chi_n)}\right)}{\chi_n\sqrt{1 - 2s\mathrm{Kn}(4 - 2\chi_n^2 s\mathrm{Kn})}}. \tag{14}$$

By means of a Galerkin projection, Eq. (8) yields the following system of periodic ordinary differential equations:

$$\mathbf{M}\frac{d\mathbf{a}}{dt} = [\mathbf{K} + \mathbf{H}\exp(it\ \mathrm{St})]\mathbf{a}. \tag{15}$$

Here, $\mathbf{a}(t)$ is an $(N \times 1)$ column vector whose $n$-th component is $a_n(t)$ and the entries of the $(N \times N)$ constant matrices **M**, **K**, **H** are defined as follows:

$$(\mathbf{M})_{jk} = \delta_{jk} - \alpha^2\langle\phi_j, \phi_k\rangle, \quad (\mathbf{K})_{jk} = i\alpha^3\langle W_0\phi_j, \phi_k\rangle - i\alpha\langle W_0\tilde{\mathcal{L}}\phi_j, \phi_k\rangle,$$

$$(\mathbf{H})_{jk} = i\alpha^3\langle W_1\phi_j, \phi_k\rangle - i\alpha(\langle W_1\tilde{\mathcal{L}}\phi_j, \phi_k\rangle - \langle\tilde{\mathcal{L}}W_1\phi_j, \phi_k\rangle),$$

where $\delta_{jk}$ is the Kronecker delta and $\langle f, g\rangle = \int_0^1 fg\,\dfrac{dr}{r}$. The energy of the velocity field associated to the approximation stream function $\hat{\psi}$ is expressed as

$$\mathcal{E}(\hat{\psi}, t) = \frac{1}{2}\int_0^1\left(\left|\frac{\partial\hat{\psi}}{\partial r}\right|^2 + \alpha^2|\hat{\psi}|^2\right)\frac{dr}{r} = \frac{1}{2}\mathbf{a}^*(t)\mathbf{M}\mathbf{a}(t), \tag{16}$$

where $\mathbf{a}^*$ denotes the Hermitian conjugate.

## 4. Stability and Space-time Evolution of an Optimal Perturbation

The time evolution of $\mathbf{a}(t)$, for any $t$, depends on the fundamental

matrix $\mathbf{G}(t)$ which satisfies the system (15) with initial conditions $\mathbf{G}(0) = \mathbf{I}$, where $\mathbf{I}$ is the $N \times N$ identity matrix. The solution for $\mathbf{a}(t)$ can be written as

$$\mathbf{a}(t) = \mathbf{G}(t)\mathbf{a}(0), \tag{17}$$

where the vector $\mathbf{a}(0)$ defines the initial conditions. Following the arguments in [3] we compute the set of eigenvalues $\{\mu_k\}_{k=1}^{N}$ of the matrix $\mathbf{G}(\mathsf{T})$, where $\mathsf{T} = 2\pi/\mathsf{St}$ is the dimensionless period of oscillations. The resulting solution is stable if all of the (complex) characteristic exponents $\gamma_k = \ln \mu_k / \mathsf{T}$ are such that $\mathsf{Re}(\gamma_k) < 0$. Note that the matrix $\mathbf{G}(\mathsf{T})$ is non-normal. For the case of steady flow one has $\mathbf{G}(t) = \exp(-t\mathbf{M}^{-1}\mathbf{K})$ and $\gamma_k$ is one of the eigenvalues of $\mathbf{M}^{-1}\mathbf{K}$. The energy growth $\mathcal{G}(t)$ of the initial perturbation defined by the vector $\mathbf{a}(0)$ is given by (see Eq. (16))

$$\mathcal{G}(\mathbf{c}, t) = \frac{\mathcal{E}(\hat{\psi}, t)}{\mathcal{E}(\hat{\psi}, 0)} = \frac{\mathbf{a}(0)^{*}\mathbf{E}(t)\mathbf{a}(0)}{\mathbf{a}(0)^{*}\mathbf{E}(0)\mathbf{a}(0)},$$

where

$$\mathbf{E}(t) = \mathbf{G}(t)^{*}\mathbf{M}\mathbf{G}(t). \tag{18}$$

The optimal initial condition $\mathbf{a}_{opt}$ which gives the maximum growth $\mathcal{G}_{opt}(t)$ attained at time $t$ satisfies the following eigenvalue problem:

$$\mathbf{E}(t)\mathbf{a}_{opt} = \mathcal{G}_{opt}(t)\mathbf{E}(0)\mathbf{a}_{opt}. \tag{19}$$

Note that $\mathcal{G}_{opt}(t)$, as a function of $t$, can be regarded as the envelope of the energy evolution of individual optimal initial conditions $\mathbf{a}_{opt}$ giving the maximum growth $\mathcal{G}_{opt}(t)$ at time $t$ (see also [9]).

### 4.1. Numerical results

We consider a perturbation with wavenumber $\alpha = 1$ and a strongly pulsatile forcing of the basic flow characterized by the ratio $K_\omega/K_0 = 2$. The characteristic exponents are plotted in Fig. 1 for a basic pulsatile flow state described by $\mathsf{Re} = 1500$, $\mathsf{Wo} = 38$ and $\mathsf{Kn} = 0.1$. For comparison

purposes, the plot of the eigenvalues of the steady flow is also shown (Wo = 0). As one can see the negative characteristic exponents indicate the stability of the flow. The eigenmodes having the highest damping in Fig. 1 are spurious due to the numerical error in computing $\mathbf{G}(T)$ by the Runge-Kutta method.

Shown in Fig. 2 for the case of the steady Poiseuille flow (Re = 3500, $\sigma = 1$, Wo = 0), is the least stable eigenvalue as a function of the Knudsen number Kn for two different values of the streamwise wavenumber ($\alpha = 0.01, 0.3$). A jump discontinuity occurs at Kn $\simeq 1/8$ implying a non-smooth behavior of the spectral properties of the Orr-Sommerfeld operator. *Depending upon the values of both* $\alpha$ *and* Kn *the slip flow can be more or less stable than the no-slip flow counterpart* (see Fig. 2). Note that this critical value of Kn is independent of wavenumber; moreover, and it can be predicted analytically from the eigenvalue relation (13). The function $F(\chi) = J_2(\chi) - 2s\mathrm{Kn}\chi J_1(\chi)$ is even and admits the following Maclaurin series expansion for $\chi << 1$,

$$F(\chi) = \frac{1}{2}\left(\frac{1}{4} - 2s\mathrm{Kn}\right)\chi^2 + \frac{1}{4!}\left(-\frac{1}{4} + 3s\mathrm{Kn}\right)\chi^4 + O(\chi^6).$$

A non-trivial root

$$\chi_0 = \sqrt{12\,\frac{8s\mathrm{Kn} - 1}{12s\mathrm{Kn} - 1}}$$

exists such that $\chi_0 < 1$ only if Kn $> 1/8s$; for Kn $< 1/8s$ all non-trivial roots exceed unity. Thus, as Kn increases starting from zero (continuum, no-slip), the least stable eigenvalue $\lambda_0 = \chi_0^2/\mathrm{Re}$ is greater than $\mathrm{Re}^{-1}$ and varies continuously until a critical value $\mathrm{Kn}_{cr} = 1/8s$ is reached. For Kn $> 1/8s$, $\lambda_0$ suddenly becomes *less* than $\mathrm{Re}^{-1}$. For the case of steady flow with Re = 3500 the plots of $\mathcal{G}_{opt}(t)$ versus $t$ are reported for Kn = 0, 0.03, 0.05, 0.1 and 0.2 in Fig. 3. One finds the largest energy growth $\mathcal{G}_{\max}$ *decreases* as Kn increases. If Kn is greater than the threshold $\mathrm{Kn}_{cr}$, then the energy growth $\mathcal{G}_{\max}$ suddenly increases as one can see

from Fig. 3 for the case of $\mathsf{Kn} = 0.2$. Thus the Orr-Sommerfeld operator for slip flow is less non-normal than the case of no-slip flow ($\mathsf{Kn} = 0$) for $\mathsf{Kn} < \mathsf{Kn}_{cr}$. The diminished shear flow at the wall due to the slip condition implies a reduction of the non-normal growth: the initial vorticity generated at the wall has less intensity as compared to the no-slip flow conditions and then the stretching of vortex tubes is less intense.

For the particular case of pulsatile flow ($\mathsf{Kn} = 0.1$, $\mathsf{Re} = 3500$ and $\mathsf{Wo} = 30$) we computed the time evolution of the flow disturbance which gives the largest energy growth (see Fig. 4). The stream function of the initial flow perturbation is given in Fig. 4(a) whose flow structures are toroidal vortex tubes. In time the mean shear stress tends to stretch the vortex tubes (Fig. 4b), so that at time $t = t_{\max} = 9.7$ (Fig. 4(c)) the energy of the flow attains its largest growth ($\mathcal{G}_{\max} \simeq 1.4$). Beyond this time the vortex tubes tend to migrate closer to the centerline, where the effectiveness of the shear stress is diminished and a decay in time occurs due to viscous effects (Fig. 4(d)).

## 5. Conclusions

In this paper, we have examined the transport and energy growth of axisymmetric disturbances in weakly rarefied flows. The flow is found to be linearly stable under all conditions; however, depending upon the values of the perturbation wavenumber $\alpha$ and $\mathsf{Kn}$ the slip flow can be more or less stable than the no-slip flow counterpart. An abrupt change in the stability properties is found to occur at the critical value of the Knudsen number $\mathsf{Kn}_{cr} = (2 - \sigma)/8\sigma$. For typical accommodation coefficients [1] this amounts to a Knudsen number of $\mathsf{Kn} \simeq 0.17 - 0.33$ which lies within the assumed slip-regime of our model. The Orr-Sommerfeld operator for slip flow is less non-normal if compared to continuum-based no-slip flow because the transient energy growth decreases as the Knudsen number increases. The optimal flow disturbance giving the largest energy growth consists of toroidal vortex tubes which are stretched and convected by the mean flow until viscous effects become dominant and the structures diffusively decay.

**Acknowledgement**

This work was supported under NSF CAREER Award CTS-0093767 (DLH).

## References

[1] E. B. Arkilic, K. S. Breuer and M. A. Schmidt, Mass flow and tangential momentum accommodation in silicon micromachined channels, J. Fluid Mech. 437 (2001), 29-43.

[2] P. G. Drazin and W. H. Reid, Hydrodynamic Stability, Cambridge University Press, New York, 1981.

[3] F. Fedele, D. L. Hitt and R. D. Prabhu, Revisiting the stability of pulsatile pipe flow, Eur. J. Mech. B Fluids 24 (2005), 237-254.

[4] X. Geng, H. Yuan, H. N. Oguz and A. Prosperetti, Bubble-based micropump for electrically conducting liquids, J. Micromech. Microeng. 11 (2001), 270-276.

[5] J. F. Hale, D. A. McDonald and J. R. Womersley, Velocity profiles of oscillating arterial flow with some calculations of viscous drag and the Reynolds number, J. Physiol. 128 (1955), 629-640.

[6] G. Em. Karniadakis and A. Beskok, Micro Flows: Fundamentals and Simulations, Springer, New York, 2002.

[7] W. W. Liou and Y. Fang, Modeling of the surface roughness effects for microchannel flows, Proc. of 33rd AIAA Fluid Dynamics Conference, Orlando, FL, June 2003, AIAA paper 2003-3586.

[8] S. C. Reddy and L. N. Trefethen, Pseudospectra of the convection-diffusion operator, SIAM J. Appl. Math. 54(6) (1994), 1634-1649.

[9] P. J. Schmid and D. S. Hennigson, Stability and Transition in Shear Flows, Springer, New York, 2001.

[10] K. P. Selverov and H. A. Stone, Peristaltically-driven channel flows with applications toward micromixing, Phys. Fluids 13 (2001), 1837-1859.

[11] J. T. Tozzi and C. H. von Kerczek, The stability of oscillatory Hagen-Poiseuille flow, J. Appl. Mech. 53 (1986), 187-192.

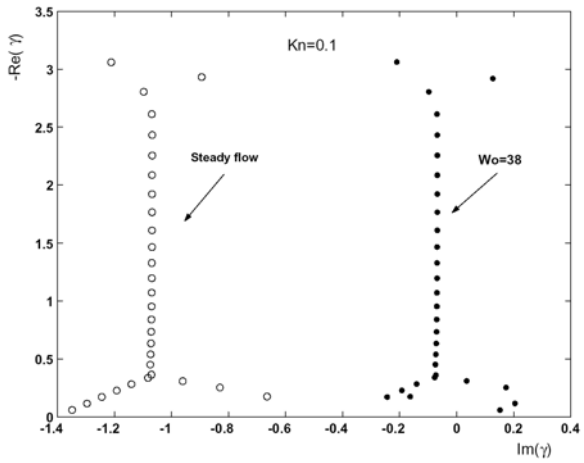


**Figure 1.** Plots of the characteristic exponents $\{\gamma_k\}_{k=1}^{N}$ for $\mathsf{Kn} = 0.1$, $\mathsf{Re} = 1500$, $\mathsf{Wo} = 38$, $K_\omega/K_0 = 2$ and wavenumber $\alpha = 1$. For comparison purposes, the plot of the eigenvalues of the steady Poiseuille flow ($\mathsf{Kn} = 0.1$) is also shown. A Galerkin expansion consisting of $N = 30$ terms was used.

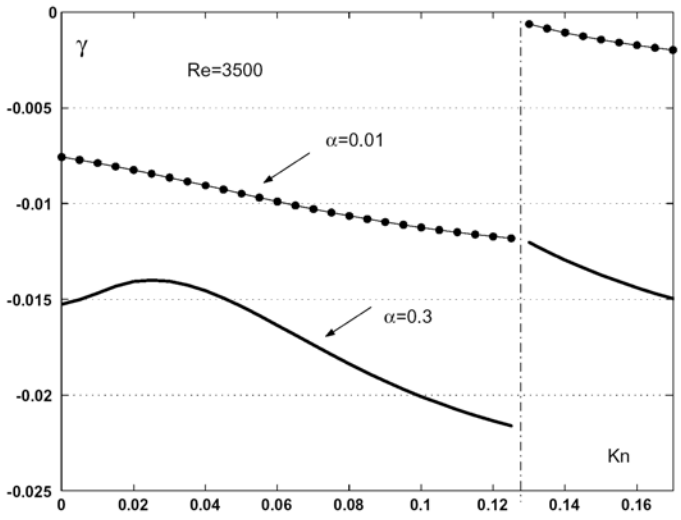


**Figure 2.** Least stable eigenvalue for the case of steady Poiseuille flow as a function of the Knudsen number for different values of the streamwise wavenumber $\alpha$ and $\sigma = 1$.

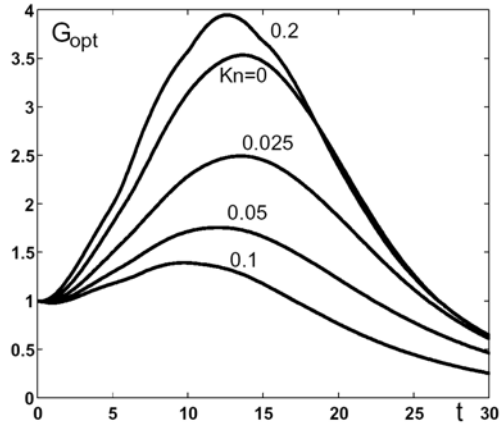


**Figure 3.** Plots of $\mathcal{G}_{opt}(t)$ for different values of the Knudsen number for $\mathrm{Re} = 3500$, $\alpha = 1$ and $\sigma = 1$ (steady flow).

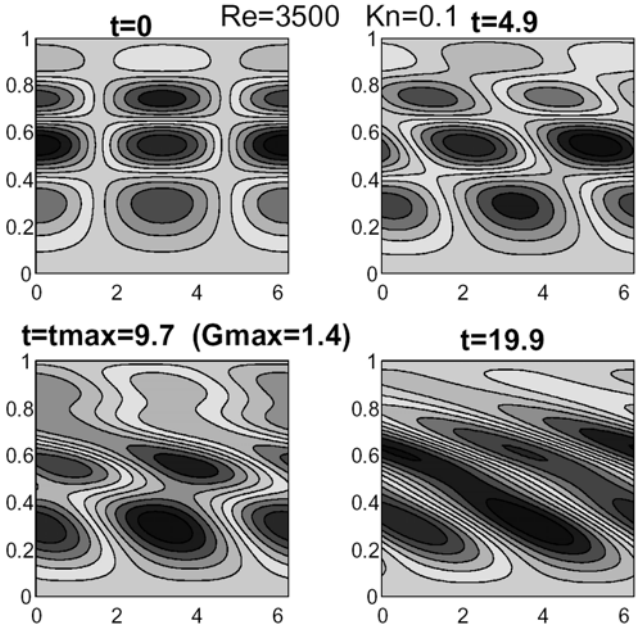


**Figure 4.** The evolution of the stream function of the optimal disturbance for $\mathrm{Re} = 3500$, $\mathrm{Kn} = 0.1$ and pulsatile flow conditions ($\mathrm{Wo} = 30$). (a) $t = 0$ (b) $t = 4.9$ (c) $t = 9.7$ (d) $t = 19.9$.